THE AMERICAN MINERALOGIST, VOL. 53, NOVEMBER–DECEMBER, 1968

ON THE LATTICE PARAMETERS AND SUPERSTRUCTURES OF PYRRHOTITES

M. E. FLEET, *Department of Geology, University of Western Ontario, London, Ontario, Canada.*

ABSTRACT

Pyrrhotites in the compositional range 50.0 to 47.7 at. % Fe have been synthesised at 700°C and low pressure and examined by X-ray diffraction procedures. Powder photographs of the quenched preparations indicate the existence of a superstructure with the hexagonal $A\sqrt{3}$, $2C$ cell (where A and C are respectively the a and c parameters of the simple NiAs cell) in pyrrhotites having more iron than 48.8 at. % Fe. Pyrrhotites more sulfur-rich than this have a superstructure with a hexagonal $2A$, $4C$ cell. Plots of the lattice parameters of the pyrrhotites studied against composition reveal a marked discontinuity at 48.8 at. % Fe. The superstructure phase boundary and the discontinuity are correlated to a structural rearrangement at this composition.

INTRODUCTION

The literature on the structure, superstructures and phase chemistry of pyrrhotites is extensive. Comprehensive résumés are available in recent publications (Wuensch, 1963, Deer, Howie and Zussman, 1962). However, in the interest of continuity, a brief account of the background information specific to the scope of this paper has been included.

The B–8 (NiAs) type structure was assigned to pyrrhotite by Alsen (1925). The nonstoichiometric nature of pyrrhotites and the regular contraction of the cell volume with increasing sulfur content of the composition has been attributed to vacancies in the iron sites of the structure (Hägg and Sucksdorff, 1933). Synthetic pyrrhotites, in the composition range 50.0 to 49.0 atomic percent iron, were found by these authors to have a superstructure with a hexagonal unit cell with $a = A\sqrt{3}$, $c = 2C$ (A and C being respectively the a and c parameters of the subcell). The superstructure was attributed by Bertaut (1956) to small displacements of the iron and sulfur atoms from their theoretical positions in the B–8 structure.

Haraldsen (1941,b) determined that pyrrhotites exhibited two solid-solid transitions above room temperature: one at 138°C, for stoichiometric FeS, (the α-transformation), common only to iron-rich pyrrhotites, and one at 325°C (β-transformation) common to all pyrrhotites. Later, Grønvold and Haraldsen (1952) concluded that the $A\sqrt{3}$, $2C$ cell was stable only below the α-transformation, where it coexisted with a pyrrhotite phase having the B–8 structure. Desborough and Carpenter (1965) reported that, for quenched pyrrhotites, a pyrrhotite phase with a hexagonal $2A$, $5C$ cell coexisted with the $A\sqrt{3}$, $2C$ phase below the α-transformation: above the α-transformation and below the β-transforma-

tion only the $2A$, $5C$ phase is present in iron-rich compositions; and above the β-transformation all pyrrhotites show a superstructure with a hexagonal $2A$, $7C$ cell. Other reported superstructures and structural modifications of pyrrhotites are: hexagonal $3A$, $2C$ (Graham, 1949); hexagonal $2A$, $4C$ (Buerger, 1947), shown subsequently to be monoclinic, pseudohexagonal (Wuensch, 1963); monoclinic, pseudohexagonal $A\sqrt{3}$, A, C, $\beta = 90.37°$ (Byström, 1945); monoclinic $2A\sqrt{3}$, $2A$, $4C$ $\beta = 89.55°$ (Bertaut, 1953). Bertaut predicted that this latter cell resulted from ordering of Fe vacancies.

Arnold (1958, 1962) and Toulmin and Barton (1964) have determined the variation in d_{102} with composition for synthetic pyrrhotites.

Experimental Details

The compositions for samples 1, 5, 7, and 9 (Table 2) were prepared from appropriate mixtures of Koch-Light Laboratories iron sponge (99.999 percent iron) and Johnson-Matthey "specpure" sulfur crystals. The iron sponge was known to be contaminated with oxygen—to the extent of 1.4 percent. Hence, for each preparation the sponge was added to a weighed silica tube, and reduced in a stream of hydrogen for 2 hours at 900°C. After allowing the tube to cool to room temperature, it was removed from the hydrogen atmosphere and reweighed. Sulfur was added and the tube was weighed once more. Thus, the weight of iron and sulfur added were determined by difference-eliminating problems arising from loss of material in transferring weighed amounts to the silica tube. After inserting a close-fitting silica rod to reduce the vapor space, the tube was sealed under vacuum. The charges were held at about 700°C for 1 day and quenched in water. The pyrrhotites in the preparations appeared homogeneous to X rays, and the compositions were lightly crushed and mixed immediately before use. The compositions for samples 2, 3, 4, 6 and 8 were prepared by homogenizing mixtures of the preparations discussed above. For each of the low pressure runs, about 100 mg of sample was contained in a sealed, evacuated silica tube, with a silica rod spacer. The charge was inserted along with a chromel-alumel thermocouple at one end of a horizontal combustion tube supported by a clampstand. The combustion tube was positioned in a horizontal tube furnace in such a way that the sample and thermocouple were in the hot-spot. In quenching the charge, the combustion tube was withdrawn from the furnace and tilted, so that the charge dropped into a container of cold water immediately adjacent to the furnace. The time required for this operation was only 2 or 3 seconds. Run durations were approximately 1 day; the recorded temperatures (Table 2) are believed accurate to ± 5°C.

Determination of Lattice Parameters

Powder diffraction films were obtained for all samples using a Jagodzinski focussing powder camera (Hofman and Jagodzinski, 1955) set up for negative, asymmetrical transmission exposures using Fe $K\alpha_1$ radiation. The samples were prepared for X-ray analysis using the mounting technique of Flörke and Saalfeld (1953). Alpine vein quartz was used as an internal standard. In determining the lattice parameters, the portion of the film in the 2θ range 35° to 90° was used, within which there are respectively 8 and 12 measurable pyrrhotite and quartz lines. The relative position of each $K\alpha_1$ line was read to the nearest 0.01 mm. Using a digital computer, a polynomial least squares regression analysis was performed on the internal standard, *i.e.* a regression of the 2θ values of α-quartz,

TABLE 1. LATTICE PARAMETERS OF STANDARD MATERIALS

Standard	Lattice parameters (determined, Å)	Probable error ($\times 10^4$, Å)	Lattice parameters (ASTM, Å)
Si	$a = 5.4305$	4	5.4301
NaCl	$a = 5.6399$	3	5.6402
Fe_3O_4	$a = 8.3959$	6	8.3963

calculated from the lattice parameters $a = 4.913$, $c = 5.404$ Å (Swanson, Fuyat and Ugrinic, 1954) against the appropriate measured film distances. The relationship, film distance against calculated 2θ, was effectively linear in the 2θ range studied: *e.g.* for sample 6, analysis of variance for simple linear regression gave:

Sum of squares of variation due to regression = 4382.25861
Residual sum of squares = 0.00111

The residual sum of squares for polynomials of degree greater than 2 were not significant. Thus a quadratic function completely described the variation and was used for all samples. 2θ values (Fe $K\alpha_1$) for the pyrrhotite lines were calculated from the regression equation, and with these data the lattice parameters were determined using the digital computer program of Mueller and Heaton (1963).

To check the accuracy of the lattice parameter method, the lattice parameters of three standard materials were determined using the same procedure as that for the pyrrhotites. The results for these materials (Si, 99.999%; NaCl, analytical reagent; Fe_3O_4 synthetic), reported in Table 1, suggest an accuracy within the range ± 0.001 Å.

The lattice parameters and observed d_{102} (the usual determinative spacing for pyrrhotite) are reported in Table 2. The parameters were calculated using only data from diffraction lines characteristic of the *B*-8 type cell: the values reported refer to this cell also. The Millerian index notation is used throughout this paper.

SUPERSTRUCTURES

Of the superstructures reported for iron-rich pyrrhotite, the $A\sqrt{3}$, $2C$ (Hägg and Sucksdorff, 1933) and $3A$, $2C$ (Graham, 1949) ones appear to be equivalent. In respect to most X-ray crystallographic phenomena, the lattices of these two superstructures would produce equivalent effects if the condition $3(h^2+hk+k^2) = (H^2+HK+K^2)$ is satisfied, where (h,k,l) and (H,K,L) relate to the $A\sqrt{3}$, $2C$ and $3A$, $2C$ cells respectively. Graham has not shown that the $3A$, $2C$ superstructure is distinct from the $A\sqrt{3}$, $2C$ one. At the same time, one can argue that the $3A$, $2C$ cell is the correct cell for the superstructure reported by Hagg and Sucksdorff. This cell is the more logical, morphologically, being formed by simple multiples of the *B*–8 cell and having a closer relation to the other reported hexagonal superstructures ($2A$, $5C$ and $2A$, $7C$): it seems that the superstructure behavior of pyrrhotites has more similarity with polytypism than with the classical superstructure

TABLE 2. LATTICE PARAMETERS OF SYNTHETIC PYRRHOTITES

Sample	Composition (at. % Fe)	Temperature of run (°C)	a (Å)	Probable error in $a(\times 10^4$, Å)	c (Å)	Probable error in $c(\times 10^4$, Å)	d_{102} (Å)
1	50.27	697	3.4451	3	5.8766	5	2.0934
2	50.02	701	3.4436	4	5.8759	7	2.0931
3	50.00	698	3.4436	3	5.8759	5	2.0933
4	49.51	698	3.4462	3	5.8554	5	2.0898
5	49.23	695	3.4471	4	5.8409	7	2.0876
6	48.89	699	3.4474	4	5.8191	6	2.0837
7	48.65	690	3.4551	3	5.7897	6	2.0805
8	48.20	698	3.4532	5	5.7695	9	2.0770
9	47.69	691	3.4495	5	5.7505	9	2.0723

behaviour exhibited by true alloys. However, the smaller, $A\sqrt{3}$, $2C$ cell will be adopted for the purposes of this paper.

Powder photographs of samples 1, 2 and 3 contained superstructure lines characteristic of the $A\sqrt{3}$, $2C$ cell. In addition several weaker, low-angle lines, not characteristic of this cell, were also evident, suggesting that either the "$A\sqrt{3}$, $2C$" cell is much larger than previously suspected or there are two distinct phases present. There is really no evidence to favor either case: precession work on crystals from sample 2 revealed several weak reflections consistent with a hexagonal $20A\sqrt{3}$, $20C$ cell for the former case and a hexagonal $20A$, $20C$ cell for the latter. Whether this superstructure development is really present in other pyrrhotites reported to have the $A\sqrt{3}$, $2C$ cell cannot be ascertained, since its apparent absence might be due to the nonresolution of the characteristic lines. The single crystal work on sample 2 and on sample 9 (below) will be reported at a later date.

Superstructure lines in powder photographs of sample 9 were not consistent with the $2A$, $7C$ cell reported for pyrrhotites of this composition quenched from high temperature. Single crystal studies revealed the presence of a hexagonal cell with $a=2A$, $c=4C$. This superstructure is similar to the one reported by Buerger (1947) in pyrrhotite from Morro Velho, Brazil: subsequent work by Wuench (1963) showed this material to be monoclinic and twinned. The pyrrhotite in sample 9 is hexagonal and apparently untwinned.

The intensities of equivalent superstructure lines of samples 1 to 6 inclusive show some correlation with composition, becoming progressively weaker and more diffuse with decreasing iron content (Figure 1). In preparing this diagram, the intensities of the stronger lines (greater than 2 percent) were determined from X-ray diffractometer analysis and those of the weaker lines were estimated from the powder photographs. The strongest of these superstructure lines (S 9) persists through to sample 6, but is not evident in sample 7.

An analogous situation is apparent in the more sulfur-rich compositions (7, 8 and 9): very weak, low-angle lines in sample 8, which appear related to the superstructure lines of sample 9, and the absence of any superstructure lines in sample 7 suggest that the development of the $2A$, $4C$ superstructure is also somewhat dependent on composition.

Discussion

The variation of lattice parameters and observed d_{102} against composition (Fig. 2) indicate a marked discontinuity at 48.8 atomic percent iron. In the direction of increasing iron content, the c parameter increases 0.015 Å and the a parameter decreases 0.008 Å. For compositions

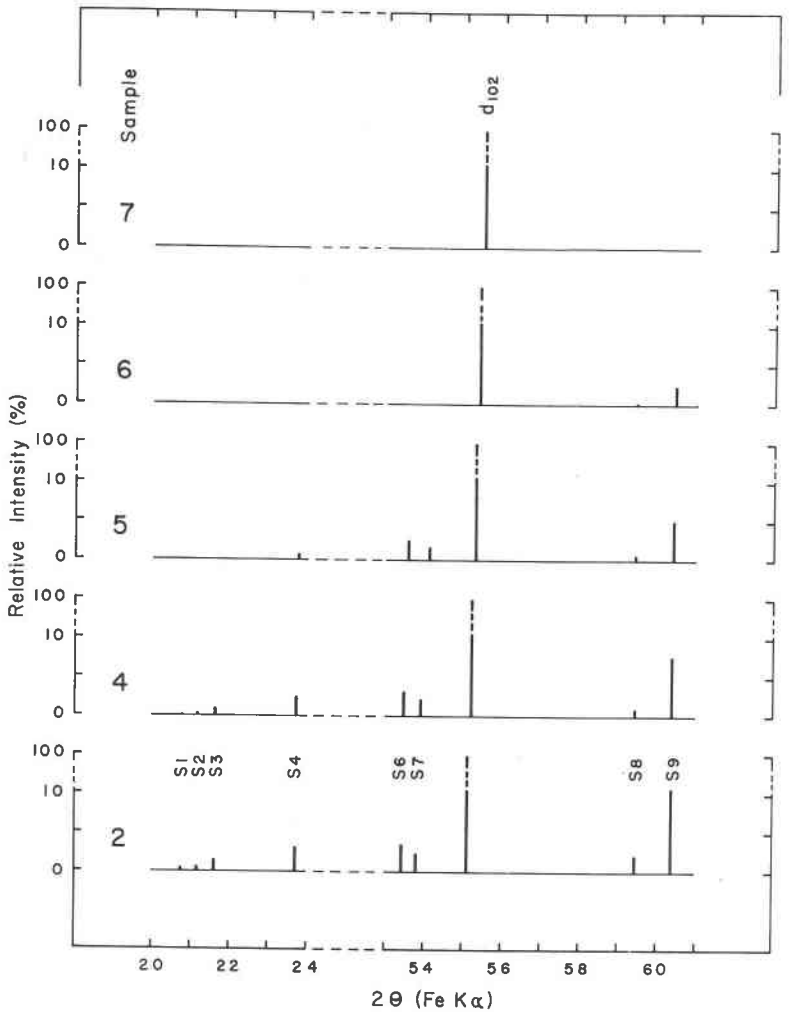

FIG. 1. Variation of the intensity of superstructure lines, in two recorded 2θ regions, with composition for pyrrhotites more iron-rich than 48.8 atomic percent iron ($S1$ and $S2$, characteristic lines of the large superstructure cell: $S3$, $S4$ and $S6$ to $S9$ inclusive, characteristic lines of the $A\sqrt{3}$, $2C$ cell being respectively the (100), (101), (203), (105), (210) and (211) reflections).

more sulfur-rich than 48.8 atomic percent iron, the variation of the parameters is similar to that obtained by earlier workers (Grønvold and Haraldsen, 1952), both parameters increasing with increasing iron content. However, on the iron-rich side of the discontinuity the a parameter shows a slight, but general, decrease. Haraldsen (1941a) reported

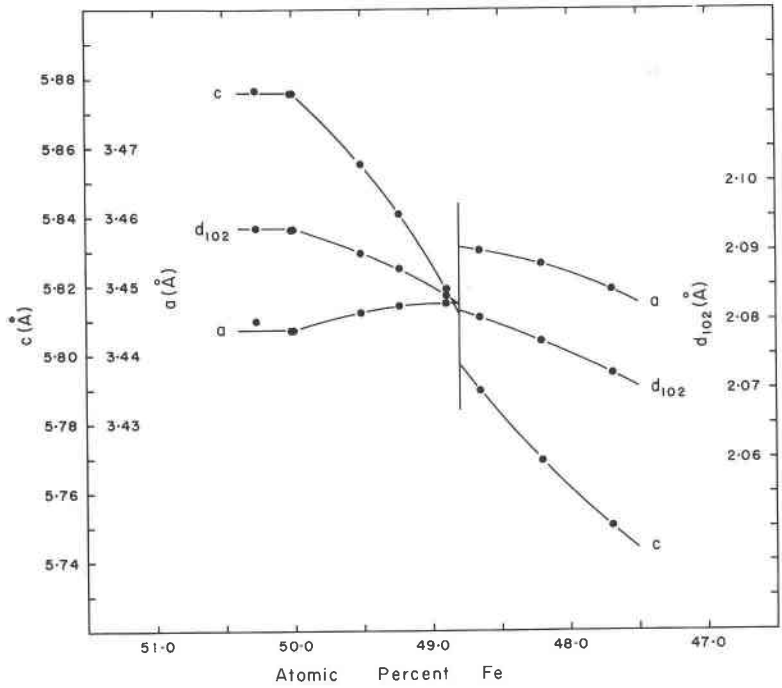

FIG. 2. Variation of lattice parameters and d_{102} of samples 1 to 9 with composition.

similar results for low temperature, synthetic pyrrhotites: except that a change in slope in the variation of the parameters was apparent, rather than a discontinuity. Later, Grønvold and Haraldsen, working on pyrrhotites annealed below the β-transformation, found no evidence to support Haraldsen's results.

The discontinuity in the variation of the d_{102} is less noticeable (0.001 Å) because the changes in the a and c parameters across the discontinuity are opposed. Comparison of the present d_{102} composition data with those of Toulmin and Barton (1964) (Fig. 3) reveals several points of interest. The average d_{102} spacing for samples 1, 2 and 3 (2.0933 Å) agrees very well with the value of 2.0932 Å reported by Toulmin and Barton for pyrrhotite in equilibrium with iron. A discontinuity in the plots of these authors is not readily apparent, possibly because the scatter of their data masks the small change to be expected, but there is some suggestion that two curves, intersecting near the composition of the discontinuity reported above, might fit the data better than a single one. Finally, (for nonstoichiometric pyrrhotites) there is a relatively large

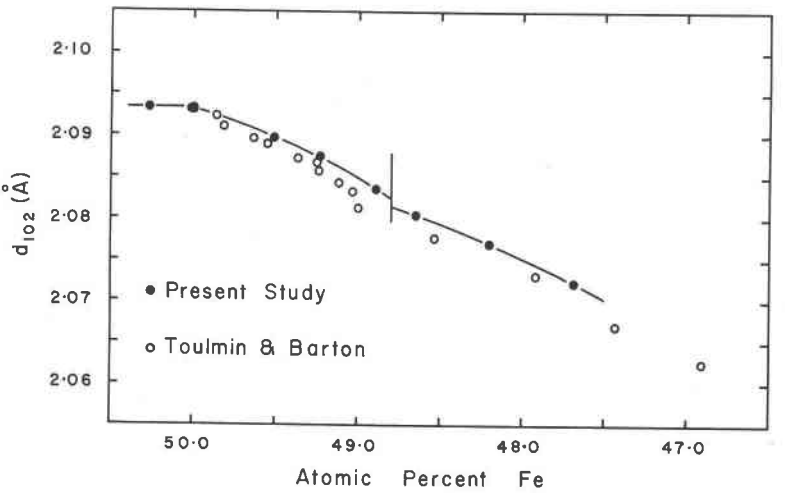

FIG. 3. Comparison of d_{102}, composition data with that of Toulmin and Barton (1964).

discrepancy between the two sets of data, the present d_{102} values being 0.001 to 0.002 Å greater than equivalent points on the Toulmin and Barton curve. It can be shown that this discrepancy is unlikely to be due to an error in composition of the present samples. The direction of the discrepancy would suggest the compositions were more iron-rich than suspected, for which a probable cause would be loss of sulfur to the vapor (oxygen contamination would result in an iron oxide phase coexisting with a pyrrhotite which would be more sulfur-rich than suspected). For sample 9, the fugacity of the sulfur vapor in equilibrium with pyrrhotite at 700°C is $10^{-3.5}$ atmospheres (Toulmin and Barton, 1964); calculations using this value show that the loss of sulfur from sample 9 (the most sulfur-rich composition investigated) would be too small to cause a discrepancy of the size reported. Also, if the difference were caused by loss of sulfur to the vapor, one might expect the two sets of data to converge at a much more sulfur-rich composition, since the fugacity of sulfur in equilibrium with pyrrhotite drops very quickly with increasing iron content. The discrepancy is probably due to different quenching procedures. The lack of information on the effects of different quenching procedures and times on pyrrhotites makes discussion of this point subjective; although it is pertinent to comment that if the charges used in the present investigation were quenched more slowly than those of Toulmin and Barton, one might expect the corresponding d_{102} to be smaller rather than greater.

The superstructure data shows that quenched iron-rich and sulfur-rich pyrrhotites are characterized by different superstructures. It is tempting to correlate the phase boundary with the discontinuity in the lattice parameters; although placement of the phase boundary to this precision (48.8 atomic percent iron) is not possible from the superstructure data alone because of the poor development of superstructures in the intermediate compositions. A phase boundary at a similar composition has been given tentative recognition by previous investigators (Haraldsen, 1941 b, and Desborough and Carpenter, 1965), but Grønvold and Haraldsen (1952) found no evidence for it in pyrrhotites equilibriated below the α-transformation.

Certainly, some structural alteration must take place across the discontinuity and this alteration probably profoundly influences the development of the superstructures. The superstructures of pyrrhotites are generally related to long-range order of the vacancies in the iron sites. The structure of the $A\sqrt{3}$, $2C$ phase has been related to small displacements of the sulfur and iron atoms from their mean position in the B–8 type structure. Clearly, it cannot be related directly to ordering of the iron vacancies since the effects of the superstructure are most evident at the stoichiometric composition. The nature of the present study permits only a generalised statement on the structure of high-temperature pyrrhotites. The results show that nonstoichiometry is accommodated in different ways by iron-rich and sulfur-rich pyrrhotites. The former probably accommodate it by a complexly distorted structure having the $A\sqrt{3}$, $2C$ or even $20A\sqrt{3}$, $20C$, cell; the distortion apparently being greatest at the stoichiometric composition. At a composition near 48.8 atomic percent iron, this structure inverts to one with the $2A$, $4C$ cell which will tolerate even greater departures from the stoichiometric composition, presumably by stabilizing iron vacancies.

ACKNOWLEDGMENTS

This work was supported by an N.R.C. Operating Grant.

REFERENCES

ALSEN, N. (1925) Röntgenographische Untersuchung der Kristallstrukturen von Magnetkies, Breithauptite, Pentlandite, Millerite und Verwandten Verbindungen. *Geol. Fören. Stockh. Forh.*, **47**, 19–72.

ARNOLD, R. G. (1958) *Pyrrhotite-pyrite equilibrium relations between 325 and 743°C*. Ph.D. Dissert., Princeton Univ.

———, (1962) Equilibrium relations between pyrrhotite and pyrite from 325 to 743°C. *Econ. Geol.*, **57**, 72–90.

BERTAUT, E. F. (1953) Contribution a l'étude des structures lacunaires: La pyrrhotine. *Acta Crystallogr.* **6**, 557–561.

BERTAUT, E. F. (1956) Structure de FeS stoechiométrique. *Bull. Soc. Franc. Minéral. Cristallogr.* **79,** 276.

BUERGER, M. J. (1947) The cell and symmetry of pyrrhotite. *Amer. Mineral.*, **32,** 411–414.

BYSTRÖM, A (1945) Monoclinic magnetic pyrites. *Ark. Kemi. Mineral. Geol.*, **19,** no. 8.

DEER, W. A., R. A. HOWIE, AND J. ZUSSMAN (1962) *Rock-Forming Minerals, 1st ed. Vol. 5*, London.

DESBOROUGH, G. A., AND R. H. CARPENTER (1965) Phase relations of pyrrhotite. *Econ. Geol.*, **60,** 1431–1450.

FLÖRKE, O. W., AND H. SAAFELD (1953) Herstellung dünner, ebener Pulverpräparate für Röntgenfeinstrukturuntersuchungen unter Verwendung von Zellulose-Kunststoffen. *Neues Jahrb. Mineral., Monatsh.* **1963,** 186–187.

GRAHAM, A. R. (1949) Artificial pyrrhotite. *Amer. Mineral.*, **34,** 462–464.

GRØNVOLD, F., AND H. HARALDSEN (1952) On the phase relations of synthetic and natural pyrrhotites ($Fe_{1-x}S$). *Acta Chem. Scand.*, **6,** 1452–1469.

HÄGG, G., AND I. SUCKSDORFF (1933) Die Kristallstruktur von Troilite und Magnetkies. *Z. Phys. Chem.*, **B22,** 444–452.

HARALDSEN, H. (1941a) Uber die Eisen (II)-Sulfidmischkristalle. *Z. Anorg. Chem.* **246,** 195–226.

——— (1941b) Uber die Hochtemperaturumwandlungen der Eisen (II)-Sulfidmischkristalle. *Z. Anorg. Chem.*, **246,** 226.

HOFMANN, E. G., AND H. JAGODZINSKI (1935) Eine neue, hochauflösiend Röntgenfeinstruktur-Anlage mit Verbessertem, Fokussierendem Monochromator und Feinfokusröhre. *Z. Metall.*, **9,** 601.

MUELLER, M. H., AND L. HEATON (1963) Determination of lattice parameters with the aid of a computer. *Argonne Nat. Lab.*, [*U. S. Clearinghouse Fed. Sci. Tech. Info.*] *Rept.* **ANL-6176.**

SWANSON. H. E., R. K. FUYAT, AND G. M. UGRINIC, (1954) Standard X-ray diffraction powder patterns. *U. S. Nat. Bur. Stand., Circ 539,* **3,** 45.

TOULMIN, P., III, AND P. B. BARTON, JR. (1964) A thermodynamic study of pyrite and pyrrhotite. *Geochim. Cosmochim. Acta.*, **28,** 641–671.

WUENSCH, B. J. (1963) On the superstructure and twinning of pyrrhotite. *Mineral. Soc. Amer. Spec. Pap.*, **1,** 157–163.

Manuscript received, November 17, 1967; accepted for publication, August 19, 1968.